CRITICAL HEAT FLUX OF R134A AND R245FA IN A 2.2 MM CIRCULAR TUBE

Cristiano Bigonha Tibiriçá, bigonha@sc.usp.br
Departamento de Engenharia Mecânica, Escola de Engenharia de São Carlos, Universidade de São Paulo, Av. Trabalhador São Carlense, 400, 13566-970, São Carlos, SP, Brasil
Laboratory of Heat and Mass Transfer (LTCM), Ecole Polytechnique Federale de Lausanne (EPFL), Station 9, Lausanne CH 1015, Switzerland.

Sylwia Szczukiewicz, sylwia.szczukiewicz@epfl.ch
Laboratory of Heat and Mass Transfer (LTCM), Ecole Polytechnique Federale de Lausanne (EPFL), Station 9, Lausanne CH 1015, Switzerland.

Gherhardt Ribatski, ribatski@sc.usp.br
Departamento de Engenharia Mecânica, Escola de Engenharia de São Carlos, Universidade de São Paulo, Av. Trabalhador São Carlense, 400, 13566-970, São Carlos, SP, Brasil.

John Richard Thome, john.thome@epfl.ch
Laboratory of Heat and Mass Transfer (LTCM), Ecole Polytechnique Federale de Lausanne (EPFL), Station 9, Lausanne CH 1015, Switzerland.

Abstract. *Critical heat flux (CHF) during flow boiling is generally related to a drastic decrease in the heat transfer coefficient and it is the maximum operational heat flux that can be achieved under safe operation. Due to such a fact, this topic has attracted great attention of the academic society dealing with boiling heat transfer and also in the industrial sector involved with the dissipation of high heat flux densities. In the specific case of high heat flux densities, micro-channel flow boiling is a promising technique for pursuing this objective. The boundary where micro-scale effects start in flow boiling is still an open issue in the literature and a 3 mm internal diameter (ID) threshold value, as suggested by Kandlikar and Grande (2003) is frequently adopted to characterize this point. Considering the needs for a better understanding of the micro/macro transition, this paper presents new experimental critical heat flux results in saturated flow boiling conditions for a macro/micro-scale tube. The data were obtained in a horizontal 2.20 mm ID stainless steel tube with heating lengths of 361 and 154 mm, R134a and R245fa as working fluids, mass velocities ranging from 100 to 1500 kg/m^{2}s, critical heat fluxes from 25 to 300 kW/m^2, exit saturation temperatures of 25, 31 and 35 ^{o}C, and critical vapor qualities ranging from 0.55 to 1. The experimental results show that critical heat flux increases with increasing mass velocity and inlet subcooling but decreases with increasing saturation temperature and heated length. The data also indicated a higher CHF for R245fa when compared with R134a at similar conditions. The experimental data were compared against the following CHF predictive methods: Katto and Ohno (1984), Shah (1987), Zhang et al. (2006) and Ong and Thome(2010). Katto and Ohno (1984) and Ong and Thome (2010) best predicted the database with a mean average error smaller than 15%. Both correlations include low and high pressure fluids in their database and worked well with this tube diameter and fluids.*

Keywords*: critical heat flux, microchannel, burnout, flow boiling,*

1. INTRODUCTION

Critical heat flux (CHF), also known in the literature as the burnout point, is generally related to a drastic decrease in the heat transfer coefficient. When heat is dissipated from a device which the imposed parameter is the heat flux, viz. microprocessors, fuel cells, spacecraft payloads and fuel elements in nuclear reactors, exceeding the CHF may result in an irreversible damage of the thermal-controlled device. Consequently, CHF is the maximum operational heat flux that can be achieved under safe operation. Due to such a fact, this topic has attracted great attention of the academic society dealing with boiling heat transfer and also of the industrial sector involved with the dissipation of high heat flux densities.

Physically, the CHF condition is observed when the liquid supply to the heated surface is covered by a layer of vapor, such that the heat is transferred from the surface to the liquid by conduction and convection through a vapor layer and, thus the wall superheating increases to a point at which the liquid is no longer able to wet the wall, and eventually radiation becomes the main heat transfer mechanism.

In convective boiling, the mechanisms related to the onset of CHF are related to the state of the working fluid. Distinct mechanisms are observed at subcooled and saturated conditions. The subcooled condition refers to when CHF is reached at the outlet of the test section while the thermodynamic vapor quality is lower than zero. Such scenarios are observed for high mass velocities, high degrees of subcooling at the inlet of the test section and low ratios of heated

length to channel diameter. The critical heat flux under saturated condition occurs when the thermodynamic vapor quality is higher than zero (but less than one) at the outlet of the test section.

For saturated CHF, the liquid film dries out near the channel outlet and this is thought to be the mechanism related to the onset of CHF. At low flow rates in small-diameter tubes, this type of CHF may be prone to occur also due to the thinner liquid film thickness as suggested by Zhang et al. (2006). For subcooled CHF, the following three mechanism have been proposed by Tong and Hewitt (1972): dryout under a vapor cloud at low mass velocities and high subcooling; bubble crowding promoting a vapour blanketing at high mass velocities; and evaporation of liquid film surrounding a slug flow bubble at low and moderate subcooling and low mass velocities. These and other theories explaining the physical mechanisms related to the achievement of critical heat flux are detailed by Maulbetsch and Griffith (1965), Kutateladze and Leont'ev (1966), Weisman and Pei (1983) and Lee and Mudawar (1988), suggested here as references for further reading.

Due to the fact that the CHF process in flow boiling is very complex, predictions rely heavily on empirical correlations based on dimensionless numbers. These dimensionless numbers include parameters that influence the CHF values measured, such as mass velocity, subcooling at the channel inlet, fluid properties, heated length and the diameter of the channel. Due to differences in the apparent mechanisms, correlations are normally separately proposed for CHF under subcooled and under saturated conditions. Most of these correlations were developed based on databases for water and macro-scale channels due to the fact that the majority of studies on CHF focused mainly on nuclear reactor applications. However, during the last decade, this scenario is changing because of the necessity to dissipate high power densities in micro-processors and power electronics and data for a wider variety of fluids and smaller diameters are now appearing in the literature.

A generalized correlation of the critical heat flux (CHF) of forced convective boiling in uniformly heated single tubes based on dimensionless numbers was proposed by Katto and Ohno (1984). This is one of the most widely used correlations and is based on a wide database and on a series of previous studies realized by the first author.

In 1987, Shah proposed a new version of his previous correlation to predict CHF during upflow in uniformly heated vertical tubes under saturated and subcooled conditions. This correlation is based on data from 62 independent sources that includes 23 fluids (water, refrigerants, cryogens, chemicals, and liquid metals), tube diameters from 0.315 to 37.5 mm, tube lengths from 1.3 to 940 times diameter, mass velocities from 4 to 29,051 kg/m^{2}s, reduced pressures from 0.0014 to 0.96 and inlet qualities from -4 to 0.85. Mean absolute errors of 16% for Shah (1987) correlation and 22.3% for Katto and Ohno's (1984) correlation were found by Shah when comparing these methods against his database.

Zhang et al. (2006) compared a database gathered from the literature for saturated and subcooled CHF against CHF predictive methods from the literature. Their database contains data only for water and covers hydraulic diameters from 0.33 to 6.22mm. A non dimensional correlation was proposed by Zhang et al. (2006) which was based on the application of the artificial neural network to identify the dominant non dimensional number for saturated CHF.

Tibiriçá et al. (2008) collected more than 1000 datapoints from the literature comprising both subcooled and saturated CHF results covering 7 fluids (water, R12, R113, R134a, R123, CO_2 and helium), mass velocities from 10.5 to 134,000 kg/m^{2}s, experimental critical heat fluxes up to 276 MW/m^2 and hydraulic diameters form 0.2 mm to 3.1 mm. This data contained only hydraulic diameters inside the range where micro-scale effects are considered (up to the 3 mm ID boundary). They concluded that Zhang et al. (2006) was the best correlation for saturated conditions with a mean average error, ε= 45% For subcooled conditions Hall and Mudawar (2000) best predicted the data with ε =22%. Tibiriçá and Ribatski (2010) also investigated the transition boundary between micro-macro scale flow boiling and observed that with their experimental data for a 2.3 mm tube no development of stratified flow pattern. This is clearly indication that at this tube diameter micro-scale effects started to exist.

Recently, Ong and Thome (2010) developed a new correlation for saturated CHF based on a previous correlation of Wojtan et al. (2006). He used a database containing 3 fluids, R134a, R245fa, R236fa covering tube diameters from 0.5 to 3.0 mm and rectangular multichannel data for equivalent diameters from 0.35 to 0.88mm. His new correlation predicted his database with ε=13% and is able to predict saturated CHF from microchannels up to the transitions limit of macro-channels.

Taking this context into account, this paper presents new experimental data for saturated CHF in a D = 2.20 mm internal diameter (ID) horizontal stainless steel tube. Tests were conducted for heated lengths of L_{heated}=154 mm and 361 mm, two working fluids, inlet subcoolings of T_{sub}=4 and 10 K, and saturation temperatures of T_{sat}=25, 31 and 35 ^{o}C. This diameter was selected based on the fact that for halocarbon refrigerants and under Earth's gravity, according to the current literature, an internal diameter of 2.2 mm seems close to the transition between micro- and macro-scale flow boiling behaviors. The main trends were identified and discussed and all the experimental results were compared against the selected predictive methods which were evaluated according to two criteria: the fraction of data predicted to within ±25%, λ, and the mean absolute error, ε.

2. EXPERIMENTS

2.1. Experimental Apparatus

The experimental setup is comprised of refrigerant and ethylene-glycol circuits. In the refrigerant circuit (see Fig. 1), starting from the condenser, the test fluid flows through the filter to the micropump. Downstream the micropump, a bypass piping line containing a needle-valve is installed so that together with a frequency controller on the micropump, the desired liquid flow rate can be set. There is a Coriolis mass flow meter and the subcooler 1 and 2 to assure that the fluid entering the pre-heater is subcooled. Just upstream the pre-heater inlet, the enthalpy of the liquid is estimated from its temperature T_1 by a 0.25mm thermocouple located at an adiabatic position outside the tube wall, and its pressure P_1 by an absolute pressure transducer.

At the pre-heater, the fluid is heated up to the desired condition for the test section inlet. The pre-heater and the test section are horizontal stainless steel tubes with an internal diameter of 2.20 mm. The internal diameter was measured using a caliper at the open end of the tube. Both are heated by applying direct DC current to their surface via two independent DC power sources and are thermally insulated. Their internal surface roughness were measured by using the non-contact, optical phase shifting and white light vertical scanning interferometry technique, which gave the root mean square (RMS) value of 0.827 μm. Downstream to the test section is located the horizontal visualization section made of a glass tube with an inner diameter of 2.2 mm, with a length of 100 mm. The pre-heater, the test section and the flow visualization section are connected through junctions made of electrical insulation material. Once the liquid leaves the test section its temperature T_2 is determined from a 0.25 mm thermocouple located on external surface at an adiabatic position. Then, the working fluid is directed to the tube-in-tube type heat exchanger where it is condensed and subcooled. The refrigerant tank containing a serpentine coil operates as a reservoir of the working fluid and is used to control the saturation pressure in the refrigerant circuit. The saturation pressure is set by adjusting the temperature of the ethylene glycol aqueous solution that flows through the serpentine coil within the refrigerant tank.

The experiments were conducted first by setting the temperature in the refrigerant tank. Once established, the mass velocity was set through a frequency controller acting on the micropump. Then, the desired subcooling in the test section was set by the power applied in the pre-heater. Heat flux was then applied to the test section to initiated two phase flow. To measure the critical heat flux, the power applied in the test section was incremented at small steps, always controlling the other parameters to keep them constant. In the current experimental campaign critical heat flux was defined when the wall temperature measured with a thermocouple located at the end of the test section reached 40 K superheating (see fig. 2). Such a procedure was used to avoid erroneous detection of the CHF due to wall temperature oscillations, which are common when working close to dryout conditions. For more details, refer to Ong and Thome (2009).

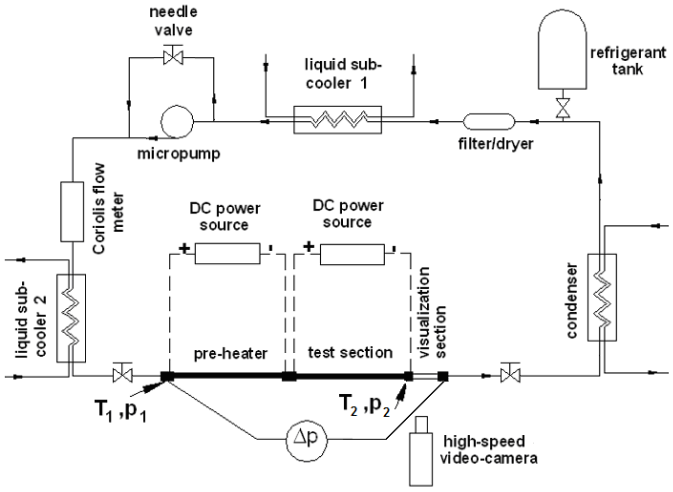

Figure 1. Test facility diagram used for CHF experiments (LTCM – EPFL).

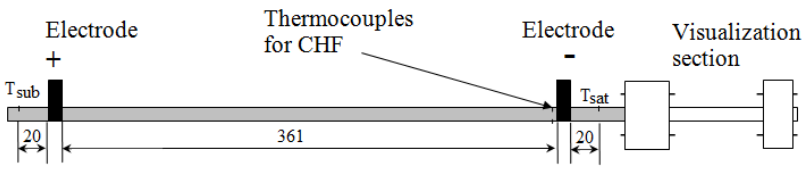

Figure 2. Test section details and thermocouple positions.

2.2. Data Reduction

The main parameters necessary for this experimental procedure are: mass velocity, G, critical heat flux, CHF and vapor quality, x. Mass velocity is the ratio between the mass flux, m, and the internal cross section area of the tube, as equation (1), where, D, is the internal tube diameter:

$$G = \frac{m}{\pi D^2} \tag{1}$$

The heat flux, q, and consequently the CHF, is the ratio between the electrical power supplied to the test section and its internal area based on the heated length, L_{heated}, where the electrical power was given by the product between the electrical current, I, and voltage supplied, V, by the DC power sources:

$$q = \frac{V \cdot I}{\pi \cdot D \cdot L_{heated}} \tag{2}$$

The exit vapor quality was determined by an energy balance over the pre-heater and the test section according to the following equation:

$$x_{out} = \frac{1}{i_{lv,out}} \left[\frac{4(P_1 + P_2)}{G\pi D^2} + \left(i_{l,in} - i_{l,out} \right) \right] \tag{3}$$

The enthalpy of the liquid at the inlet of the pre-heater, $i_{l,in}$, was estimated based on the measured temperature T_1 and pressure p_1. The liquid enthalpy and the latent heat of vaporization at the visualization section ($i_{l,out}$ and $i_{lv,out}$, respectively) were estimated based on the fluid temperature measured just downstream the test section, T_2, and assuming a saturated state. Care was taken to always read T_2 prior to dryout condition, which could lead to superheating the vapor at the outlet. In Eq. (3), P_1 and P_2 are the electrical powers supplied by the DC power sources to the heated sections.

2.3. Experimental Validation and Uncertainties

Temperature measurements were calibrated and the temperature uncertainty evaluated according to the procedure suggested by Abernethy and Thompson (1973). Uncertainties for the calculated parameters were estimated using the method of sequential perturbation according to Moffat (1988). The experimental uncertainties are listed in Table 1. Table 1 presents the uncertainties of the measured and calculated parameters, including the maximum uncertainties of the critical heat flux and vapor quality. To calculate the uncertainties of the estimated vapor qualities, it was assumed heat losses of 5%. Such a procedure was adopted since, as displayed in Fig. 3, for T_{exit}=31 °C and high mass velocities, single phase heat losses were about 5%. It should be mentioned that during two-phase flow heat losses are smaller than during single-phase flow due to a much higher internal heat transfer coefficient. In order to calculate the heat transfer coefficient uncertainties, heat losses to the environment were neglected due to the same reason abovementioned. Effects of axial heat conduction along the tube length, at the cross sections where wall temperatures were measured, were found negligible.

Table 1. Uncertainty of measured and calculated parameters.

Parameter	Uncertainty	Parameter	Uncertainty
D	20 μm	P	0.5 kPa
L	1 mm	Δp	1.0 kPa
G	2%	P_1, P_2	1%
CHF	<6%	T	0.15 °C
x	<5%		

Single-phase flow experiments were performed in order to assure the accuracy of the estimated vapor quality and evaluate the effective rate of heat losses during single-phase experiments, *(ΔE/E)*, defined as follows:

$$\left(\Delta E/E\right) = \frac{\left\{\left[\left(\pi D^2\right)/4\right] G\left(i_{out} - i_{in}\right)\right\} - \left(P_1 + P_2\right)}{P_1 + P_2} \cdot 100 \tag{4}$$

where i_{in} and i_{out} are the refrigerant enthalpies estimated at the pre-heater inlet and just downstream the test section, respectively.

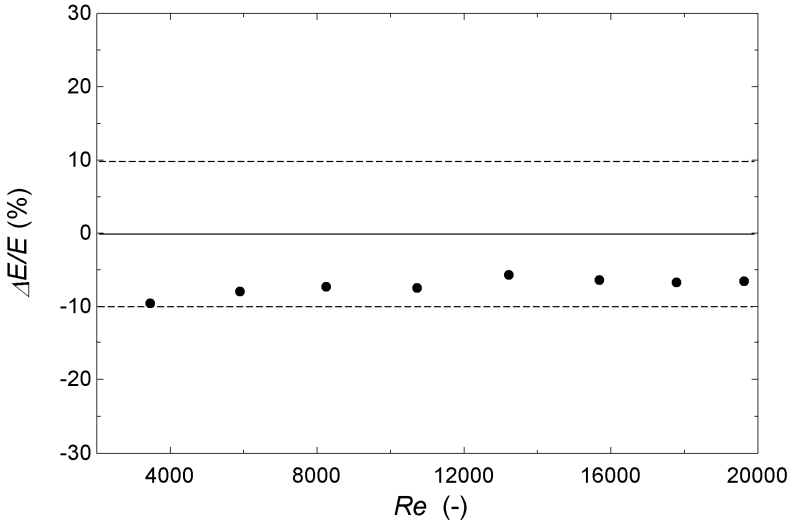

Figure 3. Single-phase energy balance for R134a including pre-heater and test section.

A flow boiling curve during a set of tests at a mass flux of 200 kg/m^{2}s for R134a is showed in fig. 4. Prior to the occurrence of the CHF, the wall superheat is smaller than 10 K. Above the value of 55 kW/m^2, a small increase in the heat flux causes a drastic increase in the wall superheating, which characterizes the CHF, here at the value of 58 kW/m^2 with 39 K superheating, ΔT_{sup}.

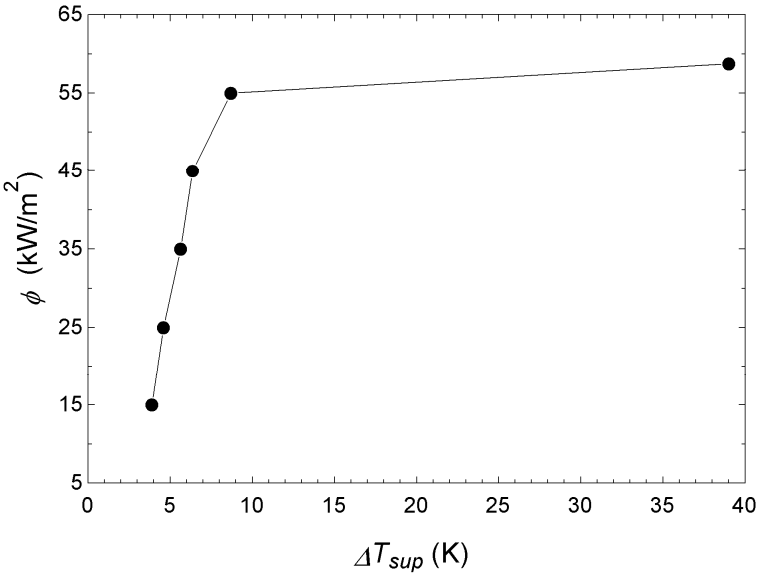

Figure 4. Wall superheating for R134a at G=200 kg/m^{2}s, T_{sat}=31°C, L_{heated}=361mm, T_{sub}=4 K.

3. RESULTS

3.1. Parameters Effect

Below, a parametric investigation of the effect of the experimental variables on the critical heat flux is presented.

Mass velocity. Figures 5 and 6 illustrate the effect of the mass velocity on CHF for R134a and R245fa, respectively. According to these figures, the CHF increases with increasing the mass velocity for all the range tested, over all subcooling, saturation temperature, and heated lengths. For R134a with L_{heated}= 361 mm it is possible to observe a small change in the slope curve starting from G=600 kg/m^{2}s. This indicates that CHF starts to occur at lower vapor qualities from this point.

Saturation temperature. For R134a in fig. 5 it is possible to observe the effect of saturation temperature on the CHF. For higher mass velocities it is very clear that at higher saturation temperature CHF decreases. This fact is also captured by most correlations and can be associated mainly with the decrease in the latent heat of vaporization with increasing saturation temperature.

Heated length. When reducing the heated length while maintaining the same inlet subcooling a higher CHF is achieved. This occurs because the heat transfer surface area is reduced and to achieve the same critical vapor quality a higher power should be applied, as demonstrated in fig. 5.

Inlet subcooling. Inlet subcooling has an effect similar to what happens when reducing the heated length. At higher subcoolings more power is necessary to achieve the same critical vapor quality, so the CHF increases with higher subcooling. However, at small subcoolings used here, the effect tends to be negligible (within experimental uncertainty).

Fluid. Figure 7 shows that R245fa has a higher CHF than R134a considering the same dimensionless parameters. This result was also observed by Ong and Thome (2010) during their experimental campaign and is also predicted by all correlations tested in this work. This can be explained due the fact that the latent heat of vaporization for the R245fa is 10% higher than that one from R134a.

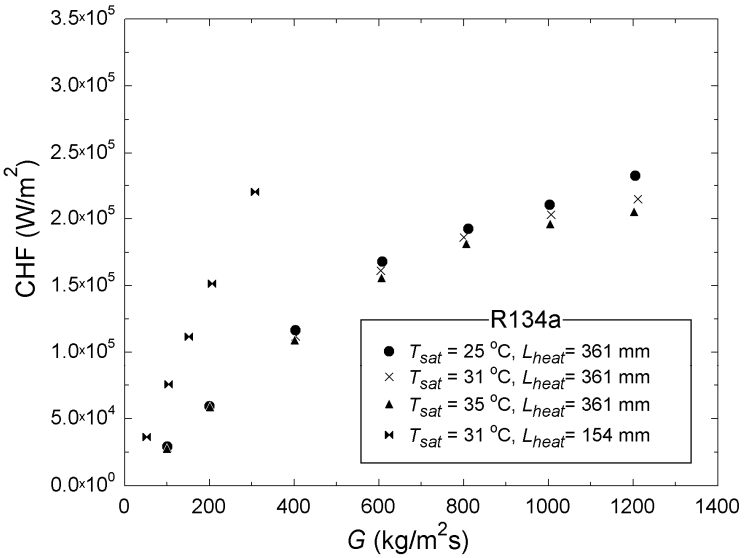

Figure 5. CHF for R134a. Effect of mass velocity, saturation temperature, and heated length.

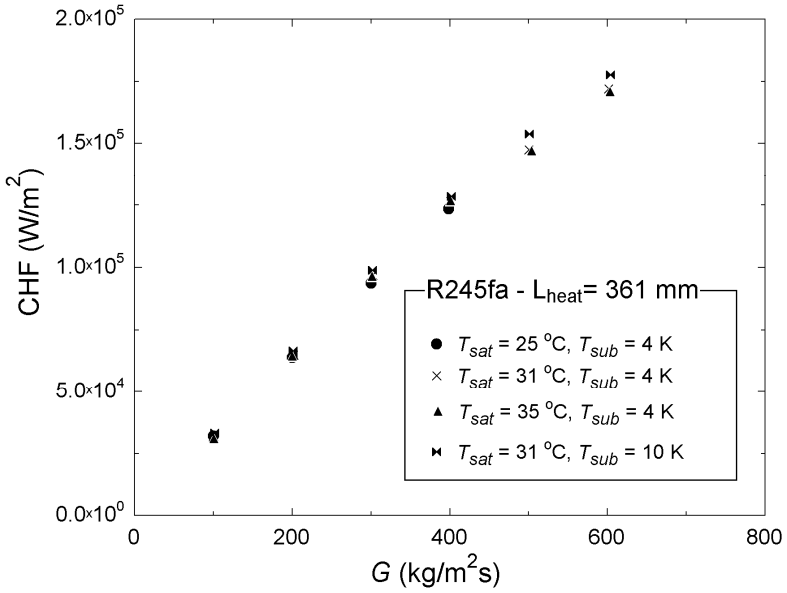

Figure 6. CHF for R245fa. Effect of mass velocity, saturation temperature and subcooling.

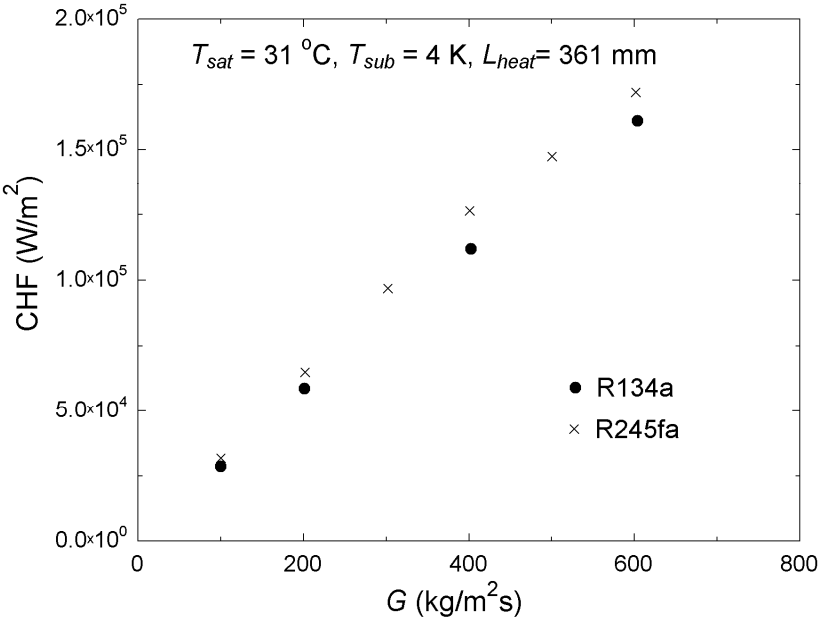

Figure 7. Comparison between CHF of R134a and R245fa.

3.2. Comparison Between The Experimental CHF and Prediction Methods

In order to evaluate the capability of CHF correlations to predict the present database, a comparison between the experimental data and four selected CHF correlations was performed. These correlations were selected considering the conclusions of the review work from Tibiriçá et al. (2008) and adding the new correlation of Ong and Thome (2010). The predictive methods are evaluated according to two criteria: the fraction of data predicted within ±25% error band, λ, and the mean absolute error, ε.

Table 2 depicts the statistics of the present comparison for the overall database. According to this table, the Katto and Ohno (1984) method worked the best followed by that of Ong and Thome (2010). Better predictions were obtained

for R245fa but for this fluid the velocity mass range tested was smaller. For both fluids, fig. 8 displays the dispersion of the experimental data compared to the correlations.

Table 2 - Statistics of the comparison between the CHF correlations and the present experimental database.

Fluid	No. of points		CHF prediction method			
			Katto and Ohno (1984)	Shah (1987)	Zhang *et al.* (2006)	Ong and Thome (2010)
R134a	32	ε (%)	10.8	24.0	14.0	14.1
		λ(%)	90.6	46.9	90.6	96.9
R245fa	22	ε (%)	2.7	25.9	18.9	13.0
		λ(%)	100.0	27.3	100.0	81.8
Total (R134a + R245fa)	54	ε (%)	7.5	24.8	16.0	13.6
		λ(%)	94.4	38.9	94.4	90.8

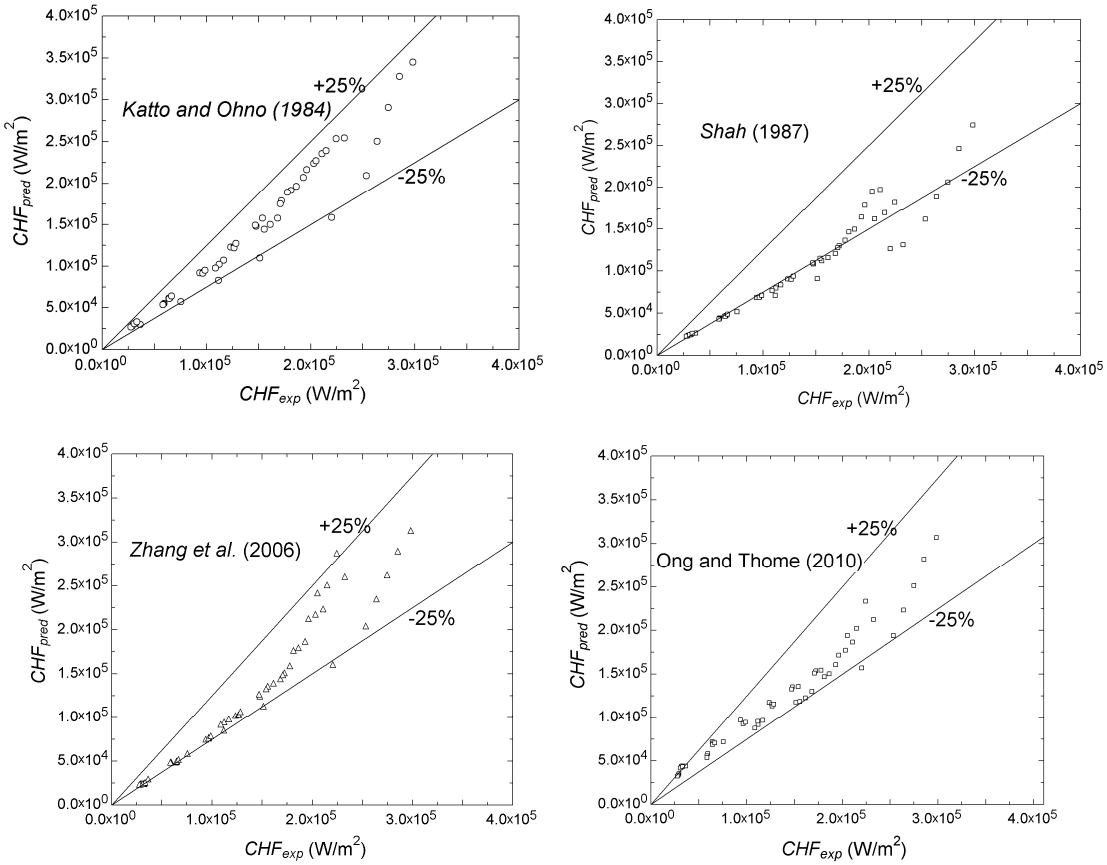

Figure 8. Comparison between the four correlations and the experimental data.

4. CONCLUSIONS

New accurate saturated critical heat flux data for R134a and R245fa in a 2.20 mm circular tube were obtained and their main behavior identified. The experimental data were parametrically analyzed and compared against predictive methods. The conclusions reached can be summarized as follows:

(1) Saturated critical heat flux increases with increasing mass velocity and slightly with inlet subcooling while it decreases with increasing saturation temperature and heated length.

(2) R245fa has a higher critical heat flux than R134a at the same experimental conditions.

(3) Comparisons between the experimental data and selected correlations from the literature indicated the best agreement with Katto and Ohno (1984) correlation with a 7.5% of mean average error and 94.4% of the data predicted with 25% uncertainty.

5. REFERENCES

Abernethy, R.B., and Thompson, J.W., 1973, "Handbook uncertainty in gas turbine measurements", Arnold Engineering Development Center, Arnold Air Force Station, Tennessee.

Hall, D. and Mudawar, I., 2000, "Critical heat flux (CHF) for water flow in tubes—II Subcooled CHF correlations", Int. J. Heat Mass Transfer, Vol. 43, pp. 2605-2640.

Kandlikar, S.G. and Grande, W.J., 2003, "Evolution of microchannel flow passages—thermohydraulic performance and fabrication technology", Heat Transfer Eng., Vol. 24, pp. 3–17.

Katto, Y. and Ohno, H., 1984, "An improved version of the generalized correlation of critical heat flux for the forced convective boiling in uniformly heated vertical tubes", Int. J. Heat Mass Transfer, Vol. 27, pp. 648-1648.

Kutateladze, S.S. and Leont'ev, A.I., 1966, Some applications of the asymptotic theory of the turbulent boundary layer, In: 3rd International Heat Transfer Conference, Chicago, USA, 3, 1-6.

Lee, C.H. and Mudawar, I., 1988, A mechanistic critical heat flux model for subcooled flow boiling based on local bulk flow conditions, Int. J. Mult. Flow, 14, 711-728.

Maulbetsch, J.S. and Griffith, P., 1965, A study of system-induced instabilities in forced-convection flows with subcooled boiling, Report N.o 5382-35, Department of Mechanical Engineering, Massachusetts Institute of Technology, USA.

Moffat, R.J., (1988). "Describing the uncertainties in experimental results", Exp. Thermal Fluid Science, Vol. 1, pp. 3-17.

Ong, C.L., and Thome, J.R. 2009, "Flow boiling heat transfer of R134a, R236fa and R245fa in a horizontal 1.030 mm. circular channel", Exp. Thermal Fluid Science, vol. 33 pp. 651-663.

Ong, C. L., Thome, J.R. 2010. "Macro-to-Microchannel Transition in Two-Phase Flow (Part 1 and 2)". Experimental Fluid Thermal Science, in review.

Shah, M., 1987, "Improved general correlation for critical heat flux during upflow in uniformly heated vertical tubes", Heat and Fluid Flow, Vol. 8, pp. 326-335.

Tibiriçá, C.B.,Felcar, H. O. and Ribatski, G., 2008, "An analysis of experimental data and prediction methods for critical heat fluxes in micro-scale channels". In: 5th European Thermal-Sciences Conference, Eindhoven. 5th European Thermal-Sciences Conference.

Tibiriçá, C.B. and Ribatski, G., 2010, "Flow boiling heat transfer of R134a and R245fa in a 2.3 mm tube", International Journal of Heat and Mass Transfer, Vol. 53, i. 11-12, pp. 2459-2468.

Weisman, J. and Pei, B.S., 1983, Prediction of critical heat flux in flow boiling at low qualities, Int. J. Heat Mass Transfer, 26, 1463-1477.

Wojtan, L., Revellin, R. and Thome, J. R., 2006, "Investigation of saturated critical heat flux in a single, uniformly heated microchannel", Exp. Thermal Fluid Sc., Vol. 30, pp. 765-774.

Zhang, W., Hibiki, T., Mishima, K. and Mi, Y., 2006, "Correlation of critical heat flux for flow boiling of water in mini-channels", Int. J. Heat Mass Transfer, Vol. 49, pp. 1058-1072.

5. RESPONSIBILITY NOTICE

The authors are the only responsible for the printed material included in this paper.